Article

Fluid Mixing in Growing Microscale Vesicles Conjugated by Surfactant Nanotubes

Max Davidson, Paul Dommersnes, Martin Markstrm, Jean-Francois Joanny, Mattias Karlsson, and Owe Orwar

J. Am. Chem. Soc., **2005**, 127 (4), 1251-1257• DOI: 10.1021/ja0451113 • Publication Date (Web): 05 January 2005

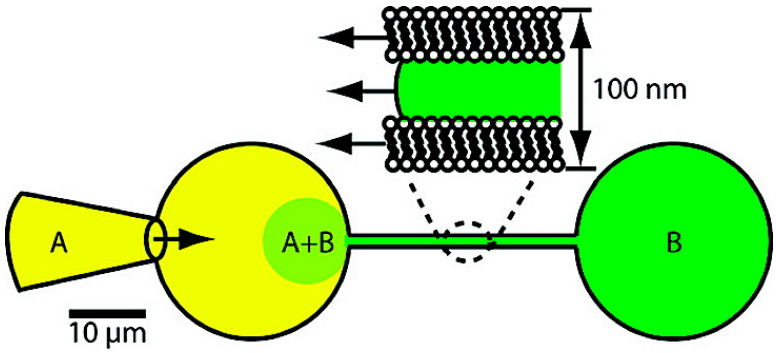

More About This Article

Additional resources and features associated with this article are available within the HTML version:

- Supporting Information
- Links to the 2 articles that cite this article, as of the time of this article download
- Access to high resolution figures
- Links to articles and content related to this article
- Copyright permission to reproduce figures and/or text from this article

View the Full Text HTML

J|A|C|S
ARTICLES
Published on Web 01/05/2005

Fluid Mixing in Growing Microscale Vesicles Conjugated by Surfactant Nanotubes

Max Davidson,[†] Paul Dommersnes,[‡] Martin Markström,[†] Jean-Francois Joanny,[‡] Mattias Karlsson,[†] and Owe Orwar*[,†,‡]

Contribution from the Department of Physical Chemistry and Microtechnology Centre, Chalmers University of Technology, SE-412 96 Göteborg, Sweden, and Institut Curie, UMR 168, 26 rue d'Ulm, F-75248 Paris Cédex 05, France

Received August 13, 2004; E-mail: orwar@phc.chalmers.se

Abstract: This work addresses novel means for controlled mixing and reaction initiation in biomimetic confined compartments having volume elements in the range of 10^{-12} to 10^{-15} L. The method is based on mixing fluids using a two-site injection scheme into growing surfactant vesicles. A solid-state injection needle is inserted into a micrometer-sized vesicle (radius 5−25 μm), and by pulling on the needle, we create a nanoscale surfactant channel connecting injection needle and the vesicle. Injection of a solvent *A* from the needle into the nanotube results in the formation of a growing daughter vesicle at the tip of the needle in which mixing takes place. The growth of the daughter vesicle requires a flow of surfactants in the nanotube that generates a flow of solvent *B* inside the nanotube which is counterdirectional to the pressure-injected solvent. The volume ratio ψ between solvent *A* and *B* inside the mixing vesicle was analyzed and found to depend only on geometrical quantities. The majority of fluid injected to the growing daughter vesicle comes from the pressure-based injection, and for a micrometer-sized vesicle it dominates. For the formation of one daughter vesicle (conjugated with a 100-nm radius tube) expanded from 1 to 200 μm in radius, the mixing ratios cover almost 3 orders of magnitude. We show that the system can be expanded to linear strings of nanotube-conjugated vesicles that display exponential dilution. Mixing ratios spanning 6 orders of magnitude were obtained in strings of three nanotube-conjugated micrometer-sized daughter vesicles.

Introduction

Control of fluid delivery inside small-dimension channels is of paramount importance in microfluidic devices, with applications in, for example, chip-based chemical analysis, drug screening, computations, and chemical kinetics.[1−4] Techniques used for fluid delivery in micrometer-sized channels include electroosmotic flow, electrochemistry, electrowetting, electrocapillary pressure, and mechanical pumping.[5−9] As a complement to these techniques, we have constructed channels in lipid bilayer systems composed of micrometer-sized vesicles connected by lipid nanotubes having a radius of 50−150 nm. To take full advantage of lipid nanotube-vesicles networks as systems for initiating and controlling chemical reactions, a way to transport materials through the nanotubes is of central importance. Such transport can be obtained by utilizing the dynamic and fluid character of the bilayer membrane. As is well-known for a system comprising two fluids separated by an interface, mechanical equilibrium requires that the interfacial tension be constant at the interface. Any gradients in tension necessarily cause interfacial transport, producing tangential forces on adjacent fluid lamina belonging to the bulk liquid phases. In other words, the spatial variation in interfacial tension creates a flow in the liquid phases on either side of the interface. Interfacial tension-driven flows are generally termed Marangoni flow, and examples of this phenomenon include spreading of films on liquid interfaces and film wetting of solid substrates.[10]

In the case of bilayer membranes, nonuniform lipid distributions can be induced by, for example, fluid convection, temperature gradients, electric fields, laser light, or mechanical means. Tangential gradients in surface tension then produce a membrane flow directed toward regions of higher surface tension. We have previously provided experimental evidence of tension-driven lipid transport using a simple model system consisting of two surface-immobilized vesicles connected by a lipid nanotube.[11] By deforming one of the vesicles using a micromanipulator-controlled carbon fiber, a gradient in membrane tension was established over the system. This results in

[†] Chalmers University of Technology.
[‡] Institut Curie.

(1) Culbertson, C.; Jacobson, S.; Ramsey, J. *J. Anal. Chem.* **2000**, *72*, 5814−5819.
(2) Dove, A. *Nat. Biotechnol.* **1999**, *17*, 859−863.
(3) Chiu, D.; Pezzoli, E.; Wu, H.; Stroock, A.; Whitesides, G. *Proc. Natl. Acad. Sci. U.S.A.* **2001**, *98*, 2961−2966.
(4) Service, R. *Science* **1994**, *265*, 316−318.
(5) Jorgenson, J.; Lukacs, K. *Anal. Chem.* **1981**, *53*, 1298−1302.
(6) Gallardo, B.; Gupta, V.; Eagerton, F.; Jong, L.; Craig, V.; Shah, R.; Abbott, N. *Science* **1999**, *283*, 57−60.
(7) Beni, G.; Tenan, M. *J. Appl. Phys.* **1981**, *52*, 6011−6015.
(8) Prins, M.; Welters, W.; Weekamp, J. *Science* **2001**, *291*, 277−280.
(9) Unger, M.; Chou, H.; Thorsen, T.; Scherer, A.; Quake, S. *Science* **2000**, *288*, 113−116.
(10) Nepomnyashchy, A.; Velarde, M.; Colinet, P. *Interfacial Phenomena and Convection*; Chapman & Hall/CRC Press: Boca Raton, FL, 2002.
(11) Karlsson, R.; Karlsson M.; Karlsson, A.; Cans, A. S.; Bergenholtz, J.; Åkerman, B.; Ewing, A. G.; Vionova, M.; Orwar, O. *Langmuir* **2002**, *18*, 4186−4190.

lipid flow from a source (vesicle in a state of lower membrane tension) to a sink (vesicle in a state of higher membrane tension). The flow of the lipid membrane is represented by a lateral translation of a cylindrical wall, translating with velocity v_n, a quantity that can be experimentally determined. This results in a moving wall driven flow of the liquid inside the tube, and thus transport of fluid between vesicles. A related method relies on formation of nanotube-integrated vesicles by adding excess membrane material to a surface-adhered vesicle. Such nanotube-integrated vesicles can be moved from one surface-immobilized vesicle to another (i.e., between the endpoints in a network) across a nanotube, thereby transporting and delivering discrete quantities of material in a controlled fashion.[12] The mobile vesicles can be emptied into the stationary vesicles at will to obtain mixing between two separate femto-to-picoliter packets of fluids.

Here we present a technique to obtain mixing between two liquids in a growing surfactant vesicle conjugated by a suspended nanotube in one end and contacted by a solid-state microinjection needle in the other end. The distal end of the nanotube is connected to a larger mother vesicle serving as lipid membrane reservoir.[13] The growth of the daughter vesicle forces membrane material from the mother to cross over the lipid nanotube to the daughter vesicle, producing a liquid flow inside the nanotube due to nonslip and viscous coupling. During inflation, the liquids from the pipet and nanotube, respectively, which can be two separate matrixes containing different solutes, will mix. We have calculated the mixing ratio of the two flows within a daughter vesicle as a function of the vesicle-nanotube system geometry, and it turns out that the liquid mixing ratio is only dependent on the relative diameters of the inflated vesicle and nanotube, but not inflation rate at the limit of no diffusion. The theoretical work is accompanied by experimental observation of the vesicle inflation parameters, with regard to daughter vesicle birth and growth as a function of pipet injection pressure. Furthermore, we have examined the respective flows from pipet and nanotube using fluorescent probes and find that this device should be useful for mixing femto-to-picoliter volumes of reactants in micrometer-scale compartments with mixing ratios spanning several orders of magnitude. The method is particularly relevant for initiation and studies of chemical reactions in confined biomimetic geometries involving small-volume transfer and few molecules. The study also provides understanding for how nanotube-vesicle networks with contents-differentiated containers can be created using well-defined materials transfer functions.

Materials and Methods

Vesicle Preparation. Vesicles were prepared from soybean lecithin dissolved in chloroform (100 mg mL^{-1}) as a stock solution. A dehydration/rehydration method previously described was used to prepare unilamellar vesicles.[13,14] In short, a droplet of lipid dispersion (1 mg mL^{-1}) was placed on a borosilicate cover slip and dehydrated in a vacuum desiccator. When the lipid film was dry, it was rehydrated with buffer solution (Trizma base 5 mM, K_3PO_4 30 mM, KH_2PO_4 30 mM, $MgSO_4$ 1 mM, EDTA 0.5 mM, pH 7.8) After a few minutes, micrometer-sized unilamellar vesicles were formed. A small sample of vesicle suspension was carried over to a drop of fresh buffer solution on a cover slip, and the vesicles were allowed to settle at the surface.

Microscopy and Fluorescence Imaging. The cover slips were placed directly on the stage of an inverted microscope (Leica DM IRB, Wetzlar, Germany). For epifluorescence illumination, the 488-nm line of an Ar+ laser (2025-05, Spectra-Physics) was used. To break the coherence and scatter the laser light, a transparent spinning disk was placed in the beam path. The light was sent through a polychroic mirror (Leica) and an objective to excite the fluorophores. The fluorescence was collected by a three-chip color CCD camera (Hamamatsu, Kista, Sweden) and recorded by using a digital video (DVCAM,DSR-11, Sony, Japan). Digital images were edited using the Adobe Premiere and Photoshop graphic software. Scion Image was used for image analysis (Scion Corp., Frederick, MD).

Micropipet-Assisted Formation of Unilamellar Networks. Fabrication of networks of nanotube-conjugated vesicles was performed as previously described.[15] With this method, networks can be produced with controlled nanotube length, angle between nanotube extensions, and vesicle container diameter. The micromanipulators (MWH-3, Narishige, Tokyo, Japan) are graded to a resolution of 0.2 μm, allowing for precise control of the *x*,*y*,*z*-position. The tapered injection micropipets were borosilicate capillaries pulled on a CO_2 laser puller instrument (model P-2000, Sutter Instrument Co., Novato, CA). A microinjection system (Eppendorf, CellTram Vario) and a pulse generator (Digitimer Stimulator DS9A, U.K.) were used to control the electroinjections.

Chemicals and Materials. Trizma base, glycerol, and potassium phosphate were from Sigma-Aldrich Sweden AB. Soybean lecithin (polar extract) was obtained from Avanti Polar Lipids, Inc. (Alabaster, AL). Chloroform, EDTA (titriplex III), magnesium sulfate, potassium dihydrogen phosphate, potassium chloride, sodium chloride, and magnesium chloride were from Merck (Darmstadt, Germany). Deionized water (Millipore Corp., Bedford, MA) was used to prepare the buffer. Alexa488-conjugated dextran was obtained from Molecular Probes (Leiden, The Netherlands).

Results and Discussion

Formation of Nanotube-Conjugated Daughter Vesicles. Tethers or nanotubes pulled from vesicles using point loads follow a first-order transition and display a force overshoot.[16] Once the tube is formed, further extension in length follows smoothly with a force $f_0 = 2\pi\sqrt{2\sigma\kappa}$, where σ is the surface tension and κ is the bending rigidity of the membrane. The required force is typically on the order of 10 pN, giving a cost of $\sim 10^{-17}$ J per 10 μm length of tube. The equilibrium radius of the tube is $a_0 = \sqrt{\kappa/2\sigma}$, which means that a vesicle with $\sigma = 0.5 \times 10^{-5}$ J m^{-1} and $\kappa = 10^{-19}$ J will have a tube with a radius of about 100 nm. The tube itself can be considered as a flexible filament with bending rigidity $k = \pi\kappa a$, which is of the order 0.6×10^{-25} J m for the values used above. A variety of experimental techniques based on micromanipulation of micrometer-sized vesicles have been developed for tether formation, including pulling with pipets[17] or optical tweezers,[18] pulling by hydrodynamic force,[19] pulling by action of polymers,[20] and pulling by action of molecular motors.[21] In all these

(12) Karlsson, R.; Karlsson, A.; Orwar, O. *J. Am. Chem. Soc.* **2003**, *125*, 8442−8443.
(13) Karlsson, M.; Nolkrantz, K.; Davidson, M.; Stromberg, A.; Ryttsen, F.; Åkerman, B.; Orwar, O. *Anal. Chem.* **2000**, *72*, 5857−5862.
(14) Criado, M.; Keller, B. *FEBS Lett.* **1987**, *224*, 172−176.
(15) Karlsson, M.; Sott, K.; Davidson, M.; Cans, A.S.; Linderholm, P.; Chiu, D.; Orwar O. *Proc. Natl. Acad. Sci. U.S.A.* **2002**, *99*, 11573−11578.
(16) Derényi, I.; Jülicher, F.; Prost, J. *Phys. Rev. Lett.* **2002**, *88*, 238101.
(17) Evans, E.; Yeung, A. *Chem. Phys. Lipids* **1994**, *73*, 39−56.
(18) Dai, J.; Sheetz, M. *Biophys. J.* **1999**, *77*, 3363−3370.
(19) Rossier, O.; Cuvelier, D.; Borghi, N.; Puech, P.; Derényi, I.; Buguin, A.; Nassoy, P.; Brochard-Wyart, F. *Langmuir* **2003**, *19*, 575−584.
(20) Kuchnir Fygenson, D.; Elbaum, B.; Shraiman, B.; Libchaber, A. *Phys. Rev. E* **1997**, *55*, 850−859.
(21) Roux, A.; Cappello, G.; Cartaud, J.; Prost, J.; Goud, B.; Bassereau, P. *Proc. Natl. Acad. Sci. U.S.A.* **2002**, *99*, 5394−5399.

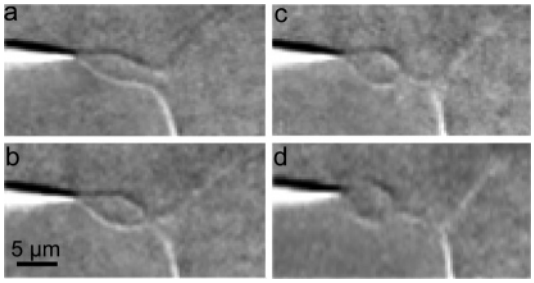

Figure 1. Formation of a nanotube-conjugated daughter vesicle. (a) A cylindrical membrane tether is pulled out. (b−d) At a critical cylinder length, the cylinder walls bend to form the daughter vesicle and nanotube. The time lapse between frames is 40 ms. The injection flow rate was 1 pL s^{-1}.

cases, the lipid membrane is adhered to the surface of the pulling object, that is, the walls of the vesicle remain intact.

In the present work, the initial step to form daughter vesicles is based on electroinjection of solid-state tips into micrometer-sized unilamellar vesicles and is quite different from the above-mentioned techniques as the tip of the injection needle is actually penetrating the membrane wall before the nanotube is pulled out.[11] Thus, after nanotube formation, the interior surface of the lipid tube is enclosing the outer surface of the tip; a liquid contact is established between the two systems. Under conditions of constant injection pressure, Nomarski differential interference contrast microscopy imaging revealed that a dilated lipid cylinder with an apical bulb is formed immediately as the pipet is pulled out from the mother vesicle; that is, there is initially no nanotube present (Figure 1a). As the pipet tip is pulled away from the mother vesicle, a small vesicle is formed at the tip of the pipet (Figure 1b). The vesicle is formed when the injection pressure is not sufficiently high to hydrodynamically maintain a large radius cylinder continuous with the vesicle body. The membrane system responds to the deformation by forming a nanotube (Figure 1c,d) because the resistance to bending is much smaller than for a stretching deformation. The integrity of the nanotube is maintained because the injection pressure is too low to force solution through the nanotube. Using the Poiseuille equation $\Delta P = Q8\eta L_t/\pi a^4$, where Q is the volumetric flowrate and L_t is the nanotube length, the pressure required to force aqueous solution at a flow rate of 1 pL s^{-1} through a 10-μm-long 100-nm-radius nanotube is ~250 kPa, a factor of 100 higher than that employed in our experiments.

Growth of a Daughter Vesicle by Hydrodynamic Injection. The growth of a daughter vesicle during injection is caused by recruiting membrane from the mother vesicle. The daughter vesicle grows by continuous injection of fluid from the microinjection system (solvent A) as well as from internal fluid (solvent B) and lipid wall material transported from the nanotube, as schematically shown in Figure 2 and displayed in the sequence of Nomarski images shown in Figure 3. The velocity of the nanotube lipid wall is determined by the rate at which the daughter vesicle grows. The total surface area of surfactant in the tube and daughter vesicle is:

$$S = 4\pi R^2 + (L - 2R)2\pi a \qquad (1)$$

where a is the radius of the nanotube, R is the radius of the daughter vesicle, and L is the distance between injection needle

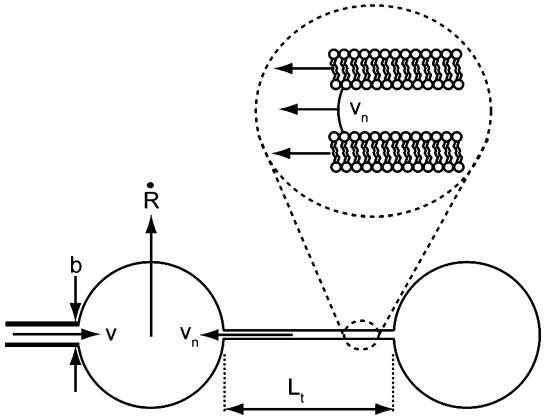

Figure 2. Schematic drawing showing geometry, flow, and growth parameters during inflation of a daughter vesicle (left compartment, injection of solvent A) at the end of a nanotube pulled from a mother vesicle (right compartment, contains solvent B).

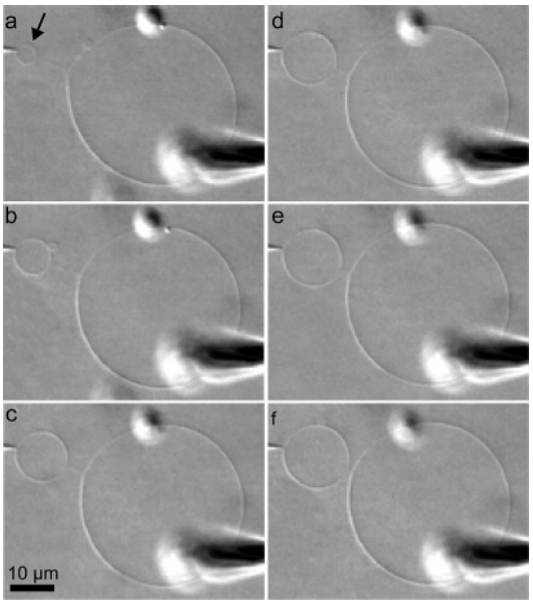

Figure 3. Time-lapse images of daughter vesicle inflation. (a) The volume of the daughter vesicle (arrow) is 0.4 pL. (b−f) The vesicle is inflated at a rate of 1 pL s^{-1} to a final volume of 10.5 pL.

and mother vesicle. The flux of surfactants going from mother vesicle to daughter vesicle is:

$$J_n = 2\pi a v_n \qquad (2)$$

where v_n is the velocity of surfactants in the nanotube, that is, the velocity of the lipid membrane wall. Conservation of surface area implies that $J_n = dS/dt$, which gives $v_n = 4(R/a)\dot{R} - 2\dot{R}$, where $\dot{R}$ is the time derivative of the vesicle radius. The last term can be neglected since $R \gg a$, hence:

$$v_n = 4\frac{R}{a}\dot{R} \qquad (3)$$

In the derivation above, we assumed that the radius of the nanotube is uniform. However, during inflation the tension in the daughter vesicle is, in general, higher than that in the mother vesicle, which results in a nonuniform tube radius. It is straightforward to show that eq 3 is still valid when the nanotube radius a varies along the tube, and the membrane wall velocity increases as the tube becomes thinner. For simplicity, in the

following we shall consider the tube radius constant. To estimate the tension gradient we approximate the hydrodynamic stress on the tube with that of a cylinder in translation motion, which corresponds to a tangential surface stress:[19]

$$\sigma_t = \frac{F}{2\pi aL} = \frac{2\eta v_n}{a \ln(L/a)} \tag{4}$$

where F is the drag on a cylinder having the same dimensions as the nanotube and moving with velocity v_n in a liquid of viscosity η. Since the Laplace pressure inside the daughter vesicle is larger than that in the mother vesicle, there will be a Poiseuille flow inside the tube $Q_P = \Delta P \pi a^4/8\eta L$. The pressure difference, ΔP, is maximal when the mother vesicle is much larger than the daughter vesicle; in this case $\Delta P \approx 2(\sigma + \Delta\sigma)/R$, where $\Delta\sigma$ is the tension difference between mother vesicle and daughter vesicle. This Poiseuille flow is superimposed on the plug flow generated by the moving walls. The tangential surface stress from Poiseuille flow is:

$$\sigma_t^P = \frac{4\eta Q_P}{\pi a^3} = \frac{a}{R}\frac{\sigma + \Delta\sigma}{L} \tag{5}$$

The tension gradient along the membrane tube is equal to the difference in tangential hydrodynamic stress on each side of the membrane:

$$\frac{\partial\sigma}{\partial z} = \sigma_t - \sigma_t^P \tag{6}$$

Equation 5 shows that the tangential stress from Poiseuille flow is small when $R \gg a$ and when the contribution to the tension difference over the tube is of the order $a/R\sigma$. Thus, the total increase in tension over the tube is approximately $\Delta\sigma \approx \sigma_t L = 2\eta v_n L/a \ln(L/a)$.

The volume flow rate of solvent B through the nanotube into the mixing vesicle is composed of a plug flow due to the moving walls and Poiseuille backflow:

$$Q_B = \pi a^2 v_n - Q_P \tag{7}$$

The total volume of solvent B in the growing vesicle is found by integrating Q_B over time, which gives:

$$V_B = 2\pi aR^2\left(1 - \frac{\sigma\pi a^3}{4\eta LQ}\right) \tag{8}$$

where $Q = 4\pi R^2\dot{R}$ is the volume growth rate of the vesicle. The total volume of the growing vesicle is:

$$V_A + V_B = \frac{4}{3}\pi R^3 \tag{9}$$

The volume flow rate of solvent A into the vesicle is $Q_A = \pi b^2 v$, where v is the constant linear flow velocity from the injector, and b is the radius of the inner channel of the tip. Experiments show that inflation of vesicles displays a linear relationship in volume growth over a large range of injection pressures. In Figure 4, this relationship is shown for injection pressures of 2, 20, and 52 hPa, using a 0.5-μm-radius tip. The nonlinearity expected at small sizes was impossible to resolve in the experiments. Equations 8 and 9 give us the volume ratio ψ between solvents A and B inside the mixing vesicle:

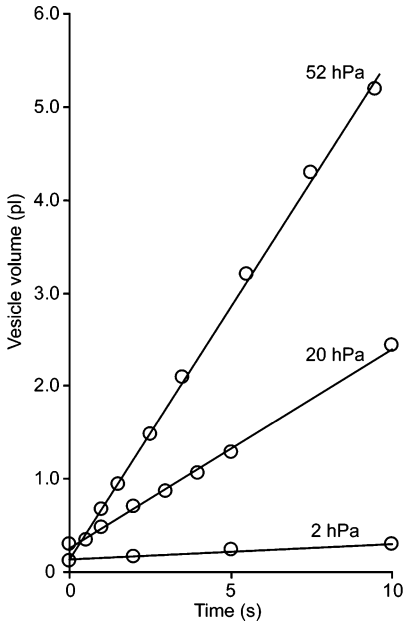

Figure 4. Increase in daughter vesicle volume with time at constant injection pressures, based on measurements of vesicle radius (see Figure 3 for setup). Each data point is an average of two experiments. Lines are simple linear fits.

$$\psi = \frac{V_B}{V_A} = \frac{3a}{2R}\left(1 - \frac{\sigma\pi a^3}{4\eta LQ}\right) \tag{10}$$

This equation is valid when $R \gg a$. For sufficiently high injection rate Q and long nanotubes, the Poiseuille backflow is small. In this case:

$$\psi = \frac{V_B}{V_A} = \frac{3a}{2R} \tag{11}$$

With a tube radius $a = 100$ nm and vesicle radius $R = 3$ μm, there will be 5% of solvent B in the mixing vesicle.

We performed experiments to verify this theory and to show that materials are quantitatively transferred from the mother vesicle across the nanotube into the growing daughter vesicle. Nanotube-conjugated daughter vesicles were formed from Alexa-dextran-loaded mother vesicles using a microinjection needle filled with nonfluorescent, isoosmolar buffer. The ratio of fluorescence intensity between the two compartments was compared after corrections for optical path length by taking the ratio between peak intensity and vesicle diameter as a measure of dye concentration. We assumed that the vesicles were attached to the surface in the low-adhesion regime and therefore treated them as spheres.[22] Figure 5 shows an experiment where Alexa dextran was transported from the mother vesicle, which contained dye corresponding to 2 mg mL^{-1}. The injection pressure was kept below that necessary to inflate a daughter vesicle ($\sim$0.5$-$1 hPa) at the tip, and therefore only a nanotube was pulled out (Figure 5a,b). Increasing the pressure to 2 hPa caused onset of daughter vesicle formation and growth, with a pipet flow rate of 0.02 pL s^{-1} during inflation (Figure 5c). Any accumulation of fluorescence in the daughter vesicle must be a

(22) Seifert, U.; Lipowsky, R *Phys. Rev. A* **1990**, *42*, 4768−4771.

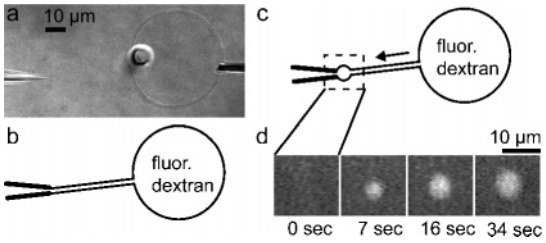

Figure 5. Nanotube-mediated transport of fluorescent dextran during formation and growth of a daughter vesicle. (a) Nomarski image of the experimental setup. (b) Schematic showing pipet tip and membrane system before formation of daughter vesicle. (c) Membrane system after formation of daughter vesicle and direction of transport flow. (d) Accumulation of the dextran in the expanding daughter vesicle.

Table 1. Measured and Calculated Mixing Ratios ψ, Vesicle Radius, and Calculated Tube Radius for Eight Vesicles

measured mixing ratio ψ (%)	vesicle radius (μm)	calculated tube radius (nm)[a]	calculated mixing ratio (%)[b]
4.8	8.0	256	3.26
2.2	7.5	110	3.48
2.2	9.3	136	2.82
5.2	5.5	191	4.75
0.5	29.0	99	0.90
0.5	30.5	109	0.86
0.1	30.5	25	0.86
1.19	25.5	203	1.02

[a] The tube radius was calculated using $a = 2R\psi/3$ (eq 11). A least-squares fit of $\psi = 3a/2R$ to the measured data gives a tube radius of 170 nm with a mean square error of 74 nm. [b] The calculated mixing ratio was derived inserting the measured vesicle radius and a tube radius of 174 nm into eq 11.

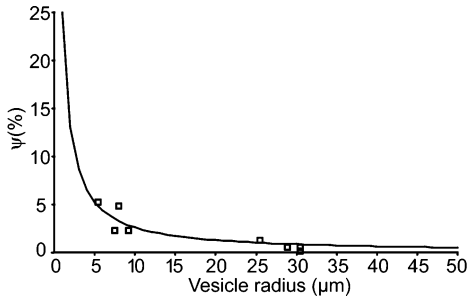

Figure 6. Mixing ratio $\psi(R)$ in formation of single daughter vesicles ($n = 8$). The line represents the least-squares fit of $\psi = 3a/2R$ to the measured data (□), giving a tube radius a of 170 nm. The mean square error was 75 nm.

result of transport across the nanotube. Figure 5d shows the advent and accumulation of Alexa dextran in the daughter vesicle, demonstrating nanotube transport. We assume that equilibration between containers by diffusion is negligible for our macromolecular solutes (see below).

In Table 1, we present the mixing ratios in percent obtained from experiments, the daughter vesicle radius in micrometers, the calculated tube radius in nanometers, and the expected mixing ratios obtained from theory calculated using eq 11 for eight vesicles in the size range of 5.5−30.5 μm in radius. Figure 6 shows the mixing ratio as a function of vesicle radius in the range of 0.5−200 μm. The best fit of eq 11 to experimental values yields a tube radius of 171 nm. As can be seen, the experimentally obtained mixing ratios are, in general, in good agreement with theoretical predictions. It is pertinent to mention a few experimental issues here. The minimal vesicle size and the precision of the technique in producing defined vesicle sizes, that is, a defined dilution, are primarily determined by the injector system but also by the manner in which vesicle growth is halted. Using the current setup, the flow is continuous and cannot be halted on demand. The lowest flow rate using a tip diameter of 0.5 μm is approximately 0.02 pL s^{-1}. At this flow rate it will take only 5−6 s to inflate a daughter vesicle to a diameter of 5 μm, at which $\dot{R}$ is 0.2 μm s^{-1}. The only way to halt vesicle growth is to position it at the substrate surface, wait for it to stick, and then gently pull the needle out. Even the most deft pair of hands will find it hard to perform this procedure in under 5 s. This explains the absence of vesicle sizes below 5 μm in Figure 6.

After their formation, the vesicles are stable (we do not observe a decrease in vesicle diameter on the time scale of the experiment). This is another indication that the pressure difference between daughter vesicle and mother vesicle is too small to create a significant Poiseuille flow, otherwise the vesicle would shrink.

In the case of pure plug flow in the nanotube, the mixing ratio between solvent A as a result of pressure injection and solvent B from the mother vesicle through the nanotube is determined by the conservation of surface area (we assume that the surfactant flow is incompressible).

Exponential Dilution and Mixing in a Plurality of Consecutively Formed Vesicles. To demonstrate serial dilution in several vesicles, we first made a daughter vesicle from a mother vesicle filled with Alexa dextran, using a pipet filled with a nonfluorescent isoosmolar buffer solution. We immobilized it on the surface, proceeded to create a second and third vesicle conjugated by nanotubes, and also immobilized these to the surface as demonstrated in Figure 7a,b. We can describe a consecutive material transfer function similar as that above for the three vesicles (which can be generalized for any given number of vesicles), and for sake of simplicity we solve it for $R_1 = R_2 = R_3$. Then we define the corresponding mixing ratios ψ_1, ψ_2, and ψ_3 for the case of formation of one, two, and three daughter vesicles. For formation of the first vesicle, one gets the mixing ratio as defined before:

$$\psi 1_1 = \frac{3a}{2R} \tag{12}$$

For two vesicles we get:

$$\psi 1_2 = \frac{3a}{R} \tag{13}$$

$$\psi 2_2 = \frac{27a^2}{8R^2} \tag{14}$$

Finally, for three vesicles we get:

$$\psi 1_3 = \frac{9a}{2R} \tag{15}$$

$$\psi 2_3 = \frac{9a^2}{R^2} \tag{16}$$

$$\psi 3_3 = \frac{9a^3}{R^3} \tag{17}$$

These equations can be generalized for any number of vesicles. Interestingly, the systems of several consecutively formed

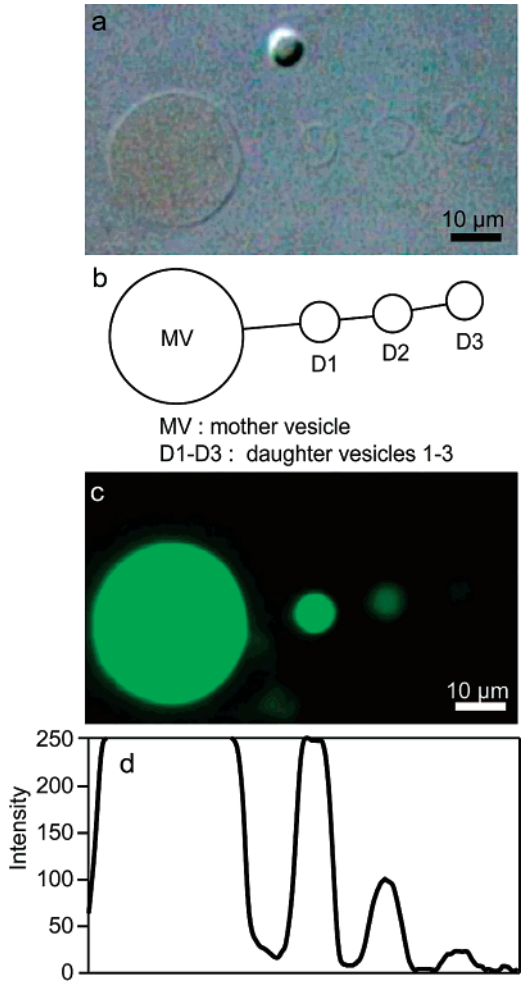

Figure 7. Serial dilution and mixing in a plurality of consecutively formed vesicles. (a) Nomarski image. (b) Schematic of the membrane compartments. (c) Corresponding fluorescence image (exposure time 1.2 s). (d) Corresponding fluorescence intensity profile.

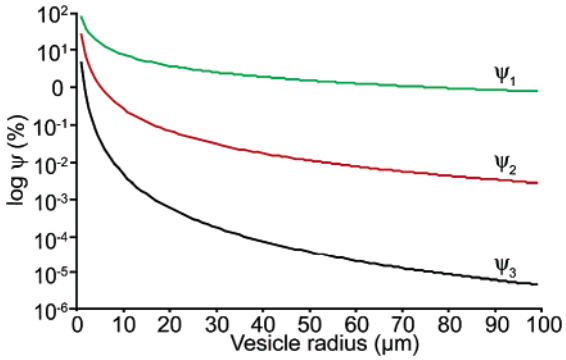

Figure 8. Calculated mixing ratio $\psi_n(R)$ in three nanotube-connected daughter vesicles as a function of vesicle radius.

vesicles behave as exponential dilution and mixing devices. Figure 8 plots log ψ_n as a function of R between 0.5 and 100 μm in diameter for the system of three conjugated vesicles (nanotube radius was set to 170 nm from the least-squares fit to the single vesicle data). ψ was calculated using eqs 15−17, where it is assumed that the three vesicles have the same radius. It can be seen that dilutions with a factor of 10^6 can be obtained between the first and last vesicle. We performed fluorescence microscopy experiments to control the validity of eqs 15−17, as shown in Figure 7c. The ratio of peak fluorescence intensity, obtained from line profiles obtained at different exposure times (Figure 7d), between the vesicles were compared pairwise. Again we made corrections for optical path length by taking the ratio between intensity peak height and vesicle diameter as a measure of concentration.

For the three consecutively formed daughter vesicles, we obtained from two separate experiments the following mixing ratios in percent: (8.6, 8.2) (1.0, 0.64), and (0.1, 0.17). The radii (in micrometers) of the respective vesicles were: (3.7, 7.7), (3.6, 5.5), and (3.8, 4). Using eqs 15−17, we found the expected mixing ratios in percent to be 12, 0.7, and 0.02. The experimentally obtained mixing ratios are in good agreement with theoretical predictions for the first two daughter vesicles but a factor of five higher than predicted for the last. We believe that the anomalous high fluorescence intensity in the latter is caused by fluorescence from membrane-associated dye.

Translocation Is Dominated by Transport and Not by Diffusion for Macromolecular Solutes. In principle, the contents in two chambers connected by a nanotube should equilibrate over time by diffusion.[23] The relaxation functions are dependent on the volume of the two vesicles, the length, and radius, respectively, of the nanotube as well as the diffusion coefficient of the solute inside the tube and the solute densities. For well-defined static geometries, these functions can be solved for a number of cases.[23] We consider here two vesicles of equal radius R connected by a tube of length L and radius a. Initially, the particle density in one of the vesicles is zero and finite in the connecting vesicle. The relaxation time is[23]

$$\tau = \frac{VL}{2D\pi a^2} \tag{18}$$

where $V = 4/3\pi R^3$ is the volume of the initially empty vesicle and all other symbols as defined above. The average time it takes for a particle to diffuse through the tube is

$$\tau_p = \frac{L^2}{D} \tag{19}$$

and after some rearrangements we get:

$$\tau = \frac{R^3}{La^2}\tau_p \tag{20}$$

Thus the equilibration time τ for the concentration in a vesicle is, in general, much larger than the diffusion time τ_p, since $R \approx L$ and $R \gg a$.

For 10 kD dextran with a diffusion coefficient of $D = 2.7 \times 10^{-7}$ cm^2 s^{-1} and typical system dimensions ($a = 150$ nm, $R = 5$ μm, $L = 7$ μm), the equilibration time is $\tau \approx 1000$ s, that is, orders of magnitude higher than the time it takes to inflate a vesicle, which typically takes a few seconds, and orders of magnitude higher than for unhindered diffusion in bulk solution. The small contribution to mass transfer by diffusion between mother and daughter vesicle is caused by the small cross section and volume element of the nanotube.

We verified experimentally that diffusion between two nanotube-conjugated vesicles is negligible under relevant time scales to form a daughter vesicle. We made daughter vesicles

(23) Dagdug L.; Berezhkovskii, A.; Shvartsman, S.; Weiss G. *J. Chem. Phys.* **2003**, *119*, 12045−12682.

from dextran-loaded mother vesicles using a buffer-filled microinjection needle. The daughter vesicle was immobilized on the glass surface, and the fluorescence intensity was measured after 0, 5, and 10 min. We performed two experiments, where the radii of the daughter vesicles were 7 and 9 μm and the nanotube lengths were 7 and 47 μm, respectively. In both cases, we observed no measurable change in intensity in the daughter vesicle over time. This demonstrates that, on the relevant time scales used for transporting materials by convection (seconds), diffusion for macromolecular solutes is not an important factor.

Conclusion

We demonstrate a novel microfluidic mixing device based on growing micrometer-scale vesicles on surfactant tubes and describe the volume ratio ψ between solvents *A* and *B* inside the mixing vesicles. The mixing ratio was found to depend only on geometrical quantities. This relation is important for understanding the mixing ratio of two or several components introduced into the vesicle from the two or several different sources.[12] In the case of formation of one daughter vesicle (conjugated with a 170-nm radius tube) expanded from 0.5 to 200 μm in radius, the mixing ratios cover almost 3 orders of magnitude. If the injection can be stopped at any instance, vesicles can be prepared with a well-defined volume of the two solutions at a given mixing ratio. We also show that in a system of several consecutively formed conjugated vesicles (nanotube radius was set to 170 nm) dilutions with a factor 10^6 can be obtained between the first and last.

The method can be used to create vesicles with different concentrations of enzymes and substrates in a controlled manner for kinetic studies by introducing an enzyme from the pipet source and substrate from the nanotube source, using the equations presented herein to determine the activity of the different species over time. Likewise, if we drive transport by injection of solution into a daughter vesicle, we can calculate the flux of particles as a function of time. This device should be useful in situations where it is desirable to mix extremely small volumes of a reactant in micrometer-scale compartments. Reaction initiation, mixing, and mass transport in biomimetic nanoscale compartments with tailored surfaces and functionalities is judged to be of considerable relevance in understanding, for example, the actions of enzymes, transporter proteins, and other biomolecules as well as properties of signaling pathways and other reaction networks. For example, these systems have a potential to provide new tools that can give unique insight into how chemical reactions occur and how fluids behave in confined geometries.[24,25] Appropriately designed, they could serve as platforms for studies of single-molecule dynamics,[26] enzyme-catalyzed reactions,[27] single-file diffusion,[28] and single-molecule sequencing and synthesis. Such systems can provide an understanding of materials transport and reactions in biological systems that occur on these length scales that, as of today, are poorly understood.[29,30] The method described herein also gives instructions for how nanotube−vesicle networks with known amounts of different species in specific containers can be constructed. In an upcoming article we will solve the hydrodynamics of these systems.

Acknowledgment. The work was supported by the Royal Swedish Academy of Sciences, the Swedish Research Council (VR), and the Swedish Foundation for Strategic Research (SSF) through a donation from the Wallenberg Foundation. O.O. acknowledges the receipt of a Rotschild-Yvette Mayent-Institut Curie Fellowship, and P.D. acknowledges the receipt of a Marie Curie Postdoctoral Fellowship. We appreciate helpful discussions with J. Prost.

JA0451113

(24) Chiu, D.; Wilson, C.; Ryttsén, F.; Strömberg, A.; Farre, C.; Karlsson, A.; Nordholm, S.; Gaggar, A.; Modi, B.; Moscho, A.; Garza-Lopez, R.; Orwar O.; Zare, R. *Science* **1999**, *283*, 1892−1895.
(25) Brody, J.; Yager, P.; Goldstein, R.; Austin, R. *Biophys. J.* **1996**, *71*, 3430−3441.
(26) LeDuc, P.; Haber, C.; Bao, G.; Wirtz, D. *Nature* **1999**, *399*, 564−566.
(27) Lu, H.; Xun, L.; Xie, X. *Scienc*e **1998**, *282*, 1877−1882.
(28) Wei, Q.; Bechinger, C.; Leiderer, P. *Science* **2000**, *287*, 625−627.
(29) Sciaky, N.; Presley, J.; Smith, C.; Zaal, K.; Cole, N.; Moreira, J.; Terasaki, M.; Siggia, E.; Lippincott-Schwartz, J. *J. Cell Biol.* **1997**, *139*, 1137−1155.
(30) Ishii, Y.; Yanagida, T. *Single Mol.* **2000**, *1*, 5−16.